Electronic Supplementary Material (ESI) for Nanoscale.

ZIF-8 engineered bismuth nanosheets arrays for direct nitrate electroreduction with boosted ammonia selectivity

Miao Chen [a], Jingtao Bi [a], Xin Huang [a, b*], Jingkang Wang [a, b], Ting Wang [a], Zhao Wang [a], Hongxun Hao [a, b, c**]

[a] National Engineering Research Center of Industrial Crystallization Technology, School of Chemical Engineering and Technology, Tianjin University, Tianjin 300072, China

[b] Collaborative Innovation Center of Chemical Science and Engineering (Tianjin), Tianjin 300072, China

[c] School of Chemical Engineering and Technology, Hainan University, Haikou 570228, China

* Corresponding author: Xin Huang, Hongxun Hao

Email address: x_huang@tju.edu.cn, hongxunhao@tju.edu.cn

Part I：Measurement of the Nitrogen-containing chemicals

1.1 Reagents

Sodium nitrate ($NaNO_3$, ≥ 99%), sodium nitrite ($NaNO_2$, 99.99%), sodium sulphate (Na_2SO_4, 99.99%), sodium hydroxide (NaOH, 99.99%), ammonium chloride (NH_4Cl, 99.998%), sodium salicylate (S3007, ≥ 99.5%), potassium sodium tartrate ($NaKC_4H_4O_6 \cdot 4H_2O$), sodium hypochlorite (NaClO, available chlorine 10-15%), sodium nitroferricyanide ($C_5FeN_6Na_2O$, ≥ 99%), p-aminobenzene sulfonamide ($C_6H_8N_2O_2S$, ≥ 99%), N- (1 naphthyl) ethylenediamine dihydrochloride ($C_{12}H_{14}N_2 \cdot 2HCl$, 98%), phosphoric acid (H_3PO_4, 85%), hydrochloric acid (HCl, 37%) were purchased from Sigma-Aldrich Chemical Reagent Co., Ltd.

1.2 Measurement of $NO_3^- - N$

The concentration of the $NO_3^- - N$ was determined by the following procedures:

The reagent (A): 8.3 ml of HCl was diluted to 100 ml to prepare 1 M HCl solution. The reagent (B): 0.8 g of NH_2SO_3H was added into 100 mL distilled water to prepare a 0.8wt% solution.

The standard $NO_3^- - N$ solution was prepared to calibrate concentration and absorbance curves by the following procedures:

a) 1000 mg$NO_3^- - N$/L of Na_2SO_4 solution: 0.6071 g $NaNO_3$ was first dried in the oven for 4 h, and then dissolved to 100 ml 0.5 M Na_2SO_4. To prepare different standard solutions, the 1000 ppm $NO_3^- - N$ solution was diluted to different concentration.

b) 10 mg$NO_3^- - N$/L in 0.5 M Na_2SO_4: 1 mL of the prepared 1000 mg$NO_3^- - N$/L Na_2SO_4 was diluted to 100 mL by adding 0.5 M Na_2SO_4 solution.

c) Standard solutions: 2, 4, 8, 12, and 16 mL of the prepared 10 mg NO_3^- - N/L Na_2SO_4 solution were diluted to 20 mL by adding 0.5 M Na_2SO_4 solution respectively. And then 1, 2, 4, 6, 8 and 10 mg NO_3^- - N/L standard solutions were obtained.

The experiments of NO_3^- - N determination followed the below procedures: 0.1 mL reagent (A) and 0.01 mL reagent (B) were added into 5 mL of the standard solutions in steps. After placing the mixed solution in a dark environment for 20 minutes, UV-vis measurement was conducted (the final absorbance= A (220 nm) - 2A (275 nm)). The concentration of the NO_3^- - N in the electrolyte was also detected by the same methods in the experiments.

1.3 Measurement of NH_4^+ - N

The concentration of NH_4^+ - N was determined by the Indophenol blue method. The reagents were prepared by the following procedures:

The reagent (A): 5 g of sodium salicylate and 5 g of potassium sodium tartrate were added into 100 mL of 1 M NaOH.

The reagent (B): 3.5 mL of NaClO was added into 100 mL distilled water.

The reagent (C): 0.1 g $C_5FeN_6Na_2O$ was added into 10 mL distilled water.

The standard NH_4^+ - N solution was prepared to calibrate concentration and absorbance curves by the following procedures:

a) 1000 mg NH_4^+ - N/L of Na_2SO_4 solution: 0.3821 g NH_4Cl was first dried in the oven for 4 h, and then dissolved to 100 ml 0.5 M Na_2SO_4.

b) 10 mg NH_4^+ - N/L in 0.5 M Na_2SO_4: 1 mL of the prepared 1000 mg NH_4^+ - N/mL Na_2SO_4 was diluted to 100 mL by adding 0.5 M Na_2SO_4 solution.

c) Standard solutions: 0.2, 0.4, 0.8, 1.2, 1.6 and 2 mL of the prepared 10 mg NH_4^+ - N/L

Na_2SO_4 were diluted to 20 mL by adding 0.5 M Na_2SO_4 solution respectively. And then 0.1, 0.2, 0.4, 0.6, 0.8 and 1 mgNH_4^+ - N/L standard solutions were obtained.

The experiments of NH_4^+ - N determination followed the below procedures: 2 mL reagent (A) was firstly added into 2 mL standard solutions, then 1 mL reagent (B) and 0.2 mL reagent (C) were added into the standard solutions in steps. After placing the mixed solution in a dark environment for 20 minutes, UV-vis measurement (the maximum λ= 655 nm) was conducted. The concentration of NH_4^+ - N in the experiments was also detected by the same methods.

1.4 Measurement of NO_2^- - N

The color reagent was prepared by adding 5 g $C_6H_8N_2O_2S$ to a mixed solution of 50 ml water and 10 ml phosphoric acid and then dissolving 0.2 g $C_{12}H_{14}N_2 \cdot 2HCl$ in the mixed solution, finally dilute above solution to 100 ml.

The standard NO_2^- - N solution was prepared to calibrate concentration and absorbance curves by the following procedures:

a) 1000 mgNO_2^- - N/L of Na_2SO_4 solution: 0.4929 g $NaNO_2$ was first dried in the glass dryer for 4 h, and then dissolved to 100 ml 0.5 M Na_2SO_4.

b) 10 mgNO_2^- - N/L in 0.5 M Na_2SO_4: 1 mL of the prepared 1000 mgNO_2^- - N/L Na_2SO_4 was diluted to 100 mL by adding 0.5 M Na_2SO_4 solution.

c) Standard solutions: 0.2, 0.4, 0.8, 1.2, and 1.6 mL of the prepared 10 mgNO_2^- - N/L Na_2SO_4 solution were diluted to 20 mL by adding 0.5 M Na_2SO_4 solution respectively. And then 0.1, 0.2, 0.4, 0.6, 0.8 mgNO_2^- - N/L standard solutions were obtained.

The experiments of NO_2^- - N determination followed the below procedures: 0.1 mL

color reagent was added into 5 mL of the standard solutions in steps. After placing the mixed solution in a dark environment for 20 minutes, UV-vis measurement (the maximum λ= 540 nm) was conducted. The concentration of the synthesized NO_2^- - N in the electrolyte was also detected by the same methods in the experiments.

Part Ⅱ： Figures

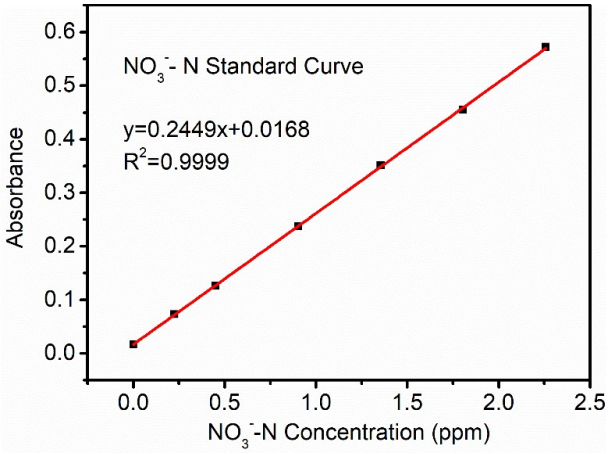

Fig. S1 Calibration curve of NO_3^- - N concentration and the absorbance of (A (220nm)-2A (270nm)). The fitting curve shows that the absorbance (A (220nm) - 2A (270nm)) and NO_3^- - N concentration in good linear relation (y = 0.2449x + 0.0168, R^2=0.9999).

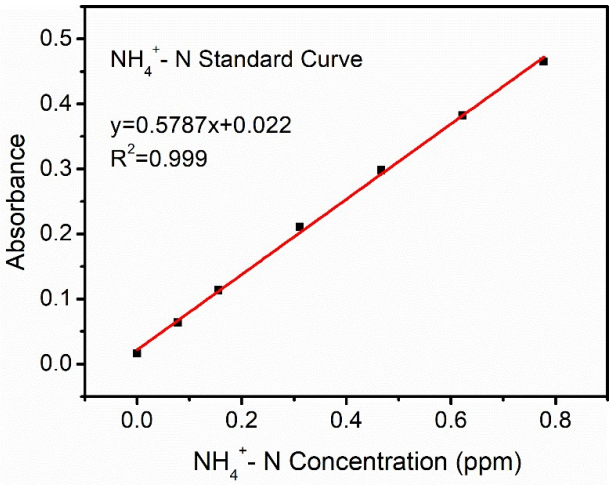

Fig. S2 Calibration curve of NH_4^+ - N concentration and the maximum absorbance. The maximum absorbance was measured at 655 nm, and the fitting curve shows good linear relation (y = 0.5787x + 0.0071, R^2=0.999).

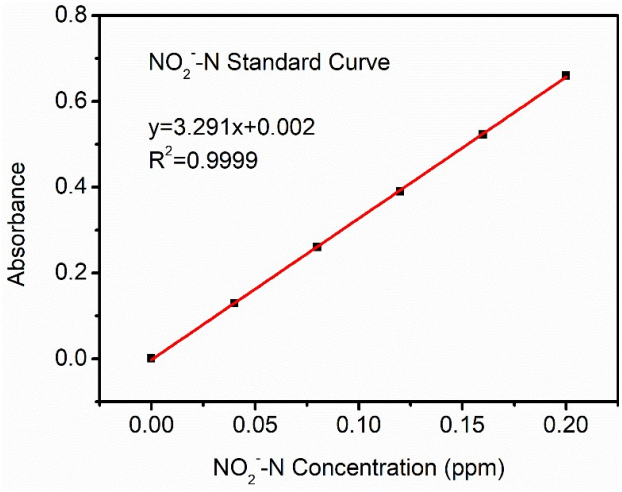

Fig. S3 Calibration curve of NO_2^- - N ion concentration and the maximum absorbance. The maximum absorbance was measured at 540 nm, and the fitting curve shows good linear relation (y = 3.291x + 0.002, R^2=0.9999).

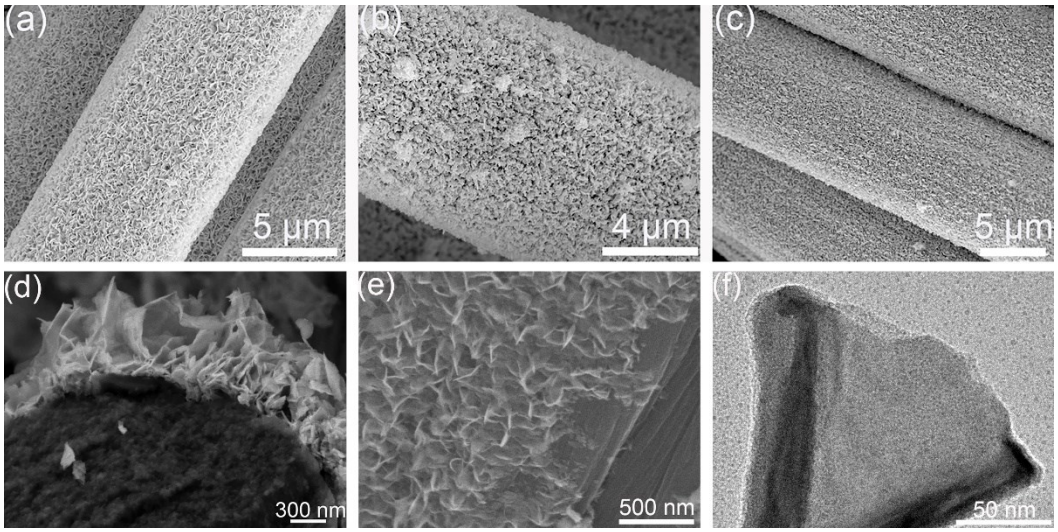

Fig. S4 (a) the SEM image of BiOI-CC, (b) the SEM image of Bi-CC electrochemical reduced from the BiOI-CC, (c) the SEM image of ZIF-8/Bi-CC, (d-e) SEM image of the interface Bi-CC, (f) TEM image of the nanosheets peeled off the ZIF-8/Bi-CC.

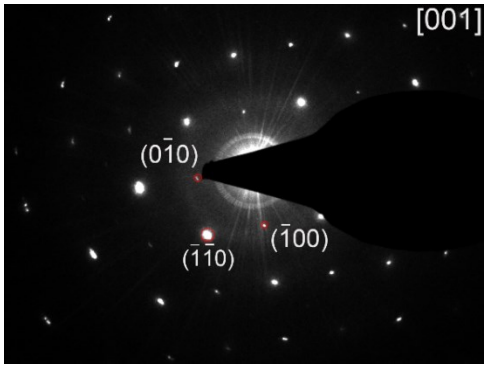

Fig. S5 SAED images of BiOI nanosheets peeled off from the carbon cloth.

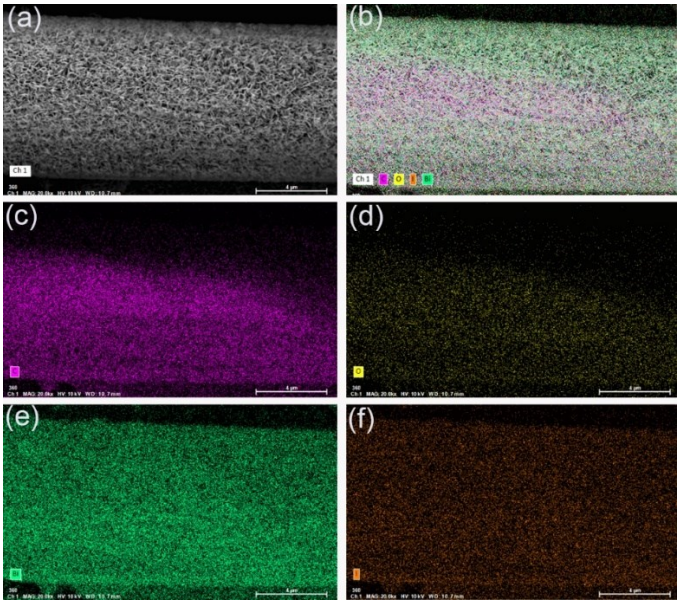

Fig. S6 The SEM-EDX images of BiOI-CC shows the even distribution of O, I and Bi.

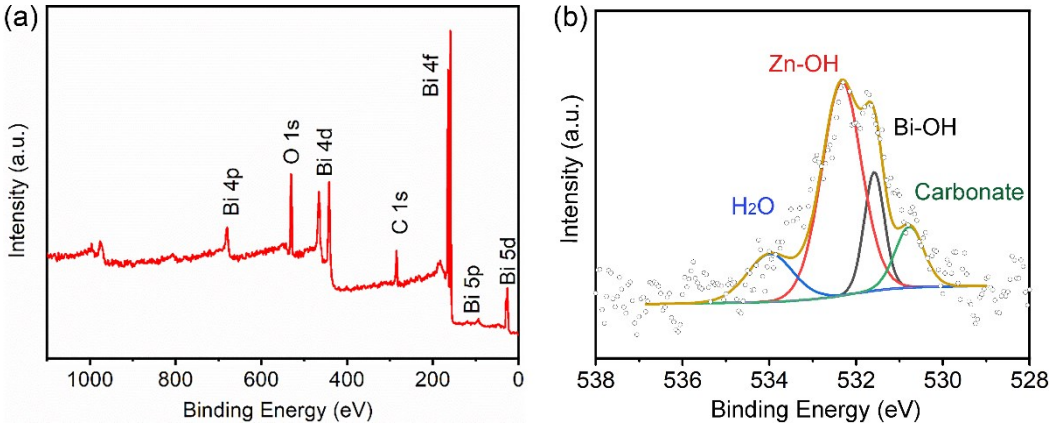

Fig. S7 (a) the Full XPS spectrum of Bi-CC transformed from BiOI-CC, (b) the O1s spectrum of ZIF-8/Bi-CC.

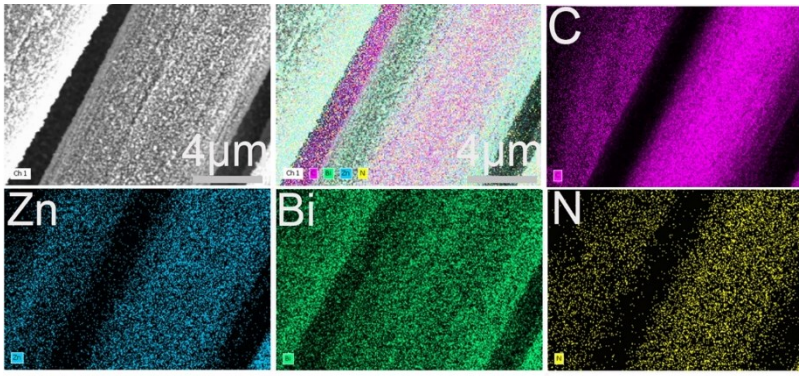

Fig. S8 The SEM-EDX images of ZIF-8/Bi-CC shows the even distribution of C, N, Zn and Bi.

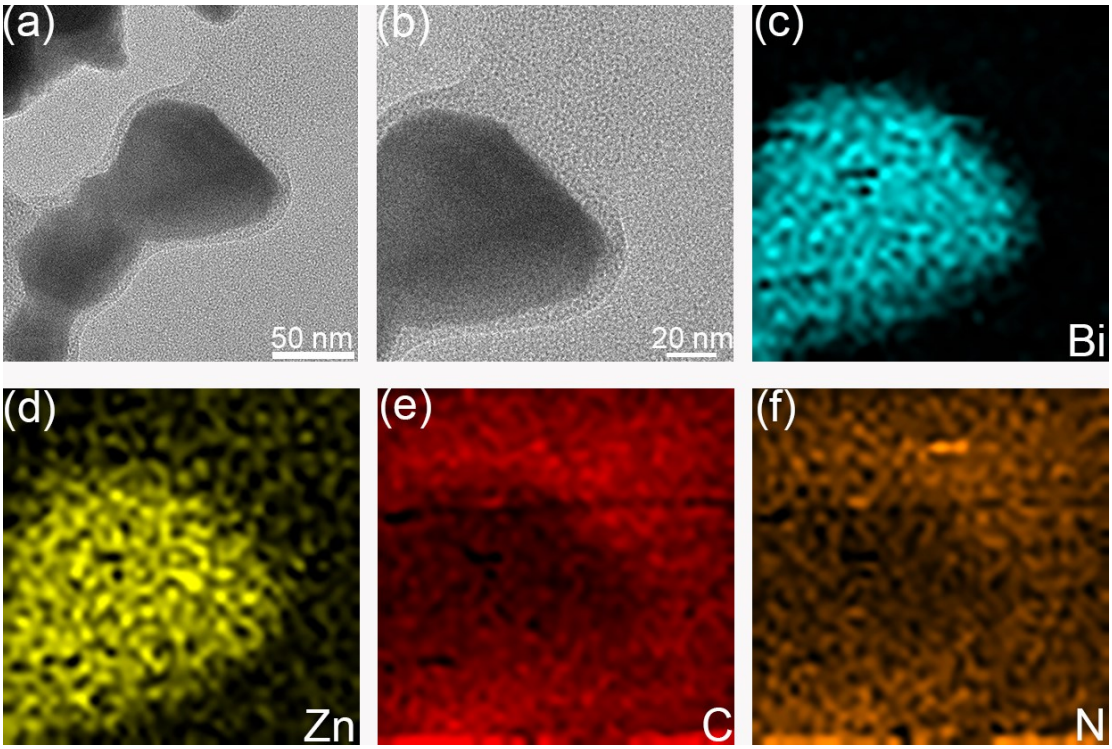

Fig. S9 TEM-Mapping images of the nanosheets peel off the ZIF-8/Bi-CC.

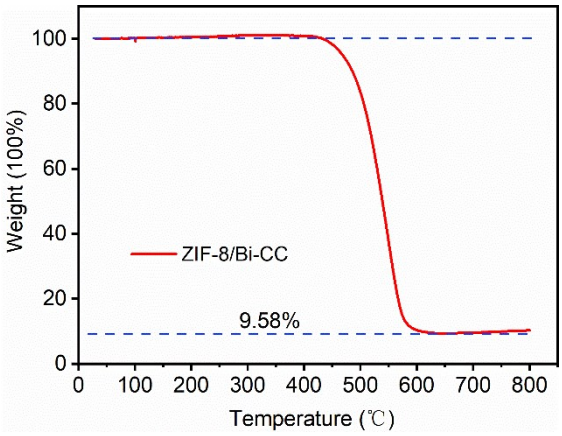

Fig. S10 Weight loss analysis of ZIF-8/Bi-CC by thermogravimetric analysis (TGA) in air.

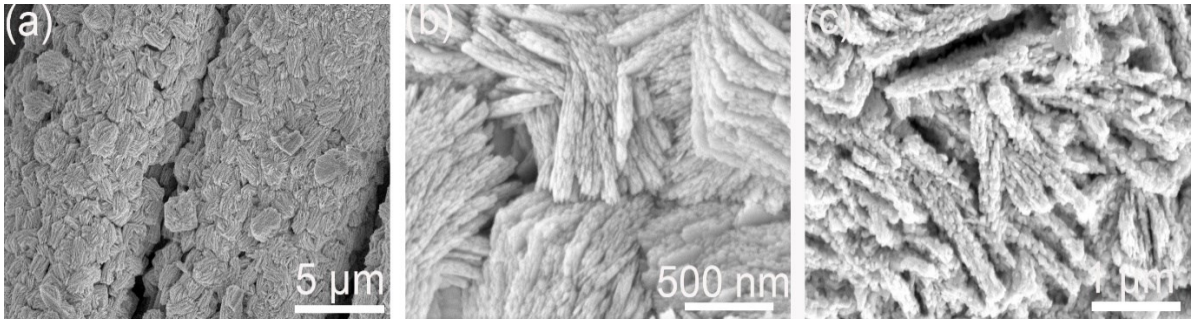

Fig. S11 (a), (b) SEM images of BiOCl-CC with different scales and (c) SEM image of the Bi-CC electrochemical reduced from the BiOCl-CC.

Fig. S12 (a), (b) SEM images of BiOBr-CC with different scales and (c) SEM image of the Bi-CC electrochemical reduced from the BiOBr-CC.

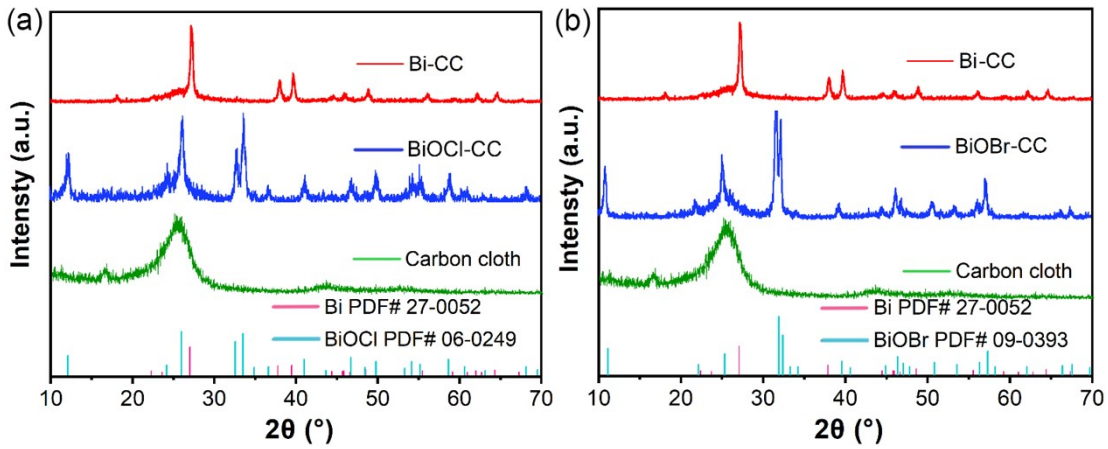

Fig. S13 (a) The XRD spectra of carbon cloth, BiOCl-CC, and Bi-CC, respectively; (b) The XRD spectra of the carbon cloth, BiOBr-CC, and Bi-CC, respectively.

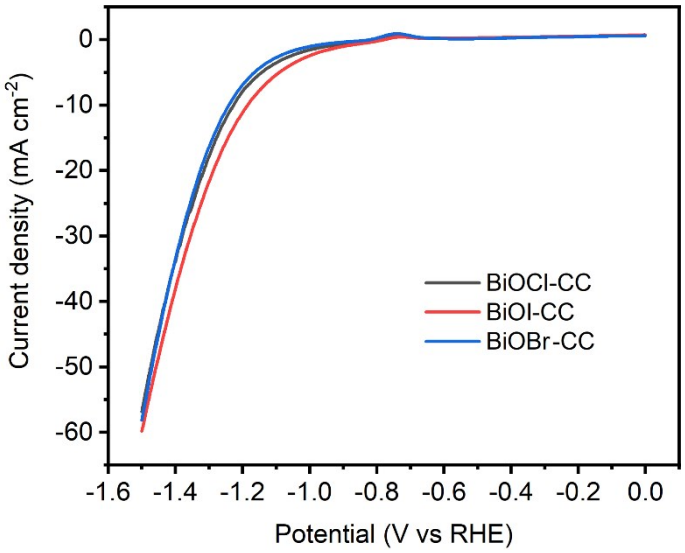

Fig. S14 LSV curves of the obtained Bi-CC by the electroreduction from different precursors in 0.5 M Na_2SO_4.

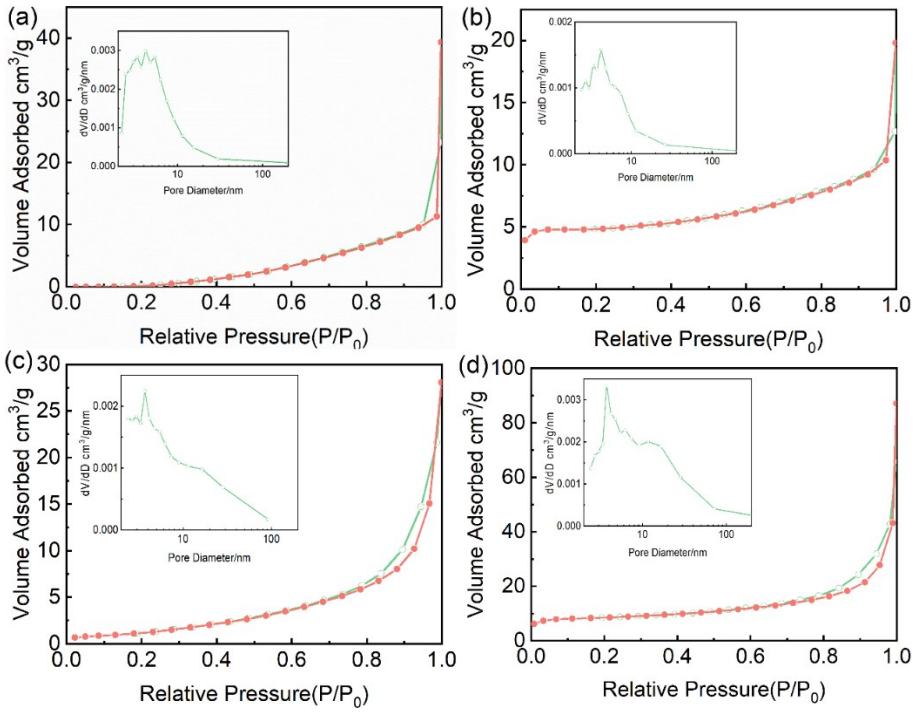

Fig. S15 N_2 adsorption-desorption isotherms and pore size distributions (desorption branch) of carbon cloth, ZIF-8/CC, Bi-CC and ZIF-8/Bi-CC.

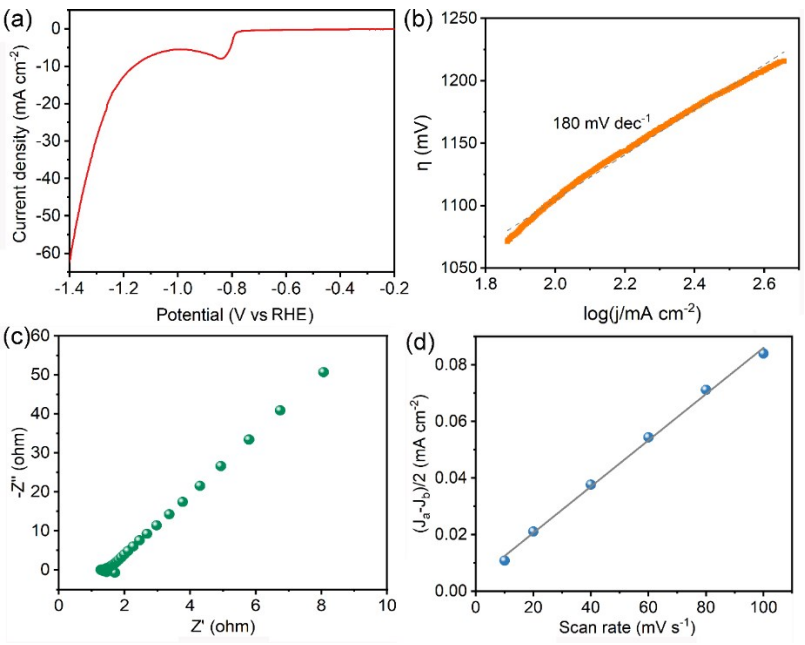

Fig. S16 Characterization of the HER electrocatalytic activity of ZIF-8/CC: (a) LSV curve with IR corrected in 0.5 M Na_2SO_4 within 50 ppm NO_3^- - N; (b) corresponding Tafel plot derived from (a); (c) electrochemical impedance spectroscopy curves of ZIF-8/CC were performed in 0.5 M Na_2SO_4 within $0.01-10^5$ Hz at open circuit voltage; (d) charge current differences plotted against a scan rate in the ZIF-8/CC.

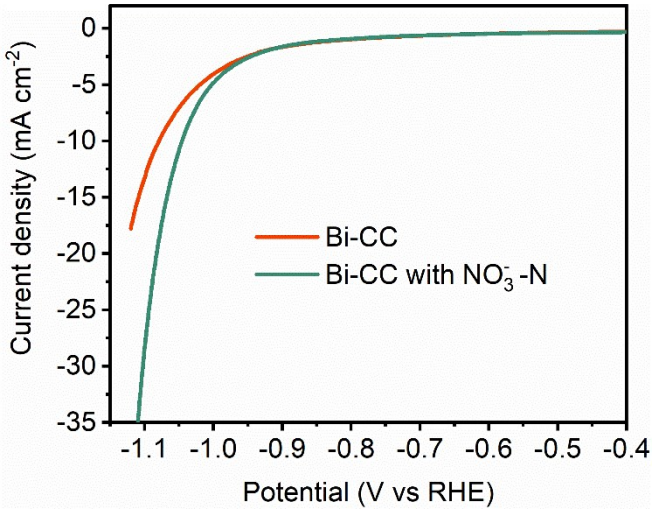

Fig. S17 LSV curves of the obtained Bi-CC with IR corrected in 0.5 M Na_2SO_4 with and without of the addition of 50 ppm NO_3^- - N.

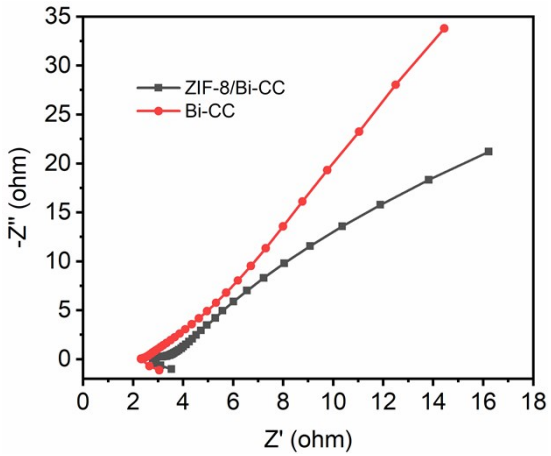

Fig. S18 Electrochemical impedance spectroscopy curves of Bi -CC and ZIF-8/Bi-CC were performed in 0.5 M Na_2SO_4 (pH=3±0.2) within $0.01-10^5$ Hz at open circuit voltage with an amplitude of 10 mV.

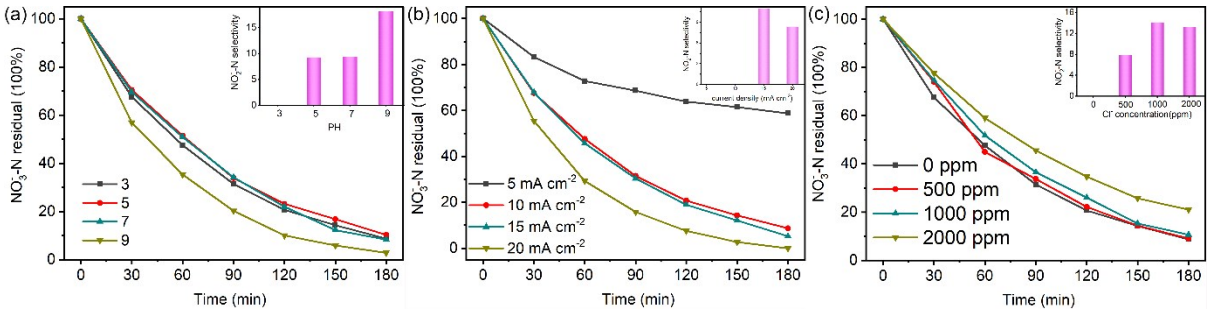

Fig. S19 The NO_3^- - N residual and NO_2^- - N selectivity of different reaction parameters: (a) PH, (c) current density, (d) Cl^- concentration.

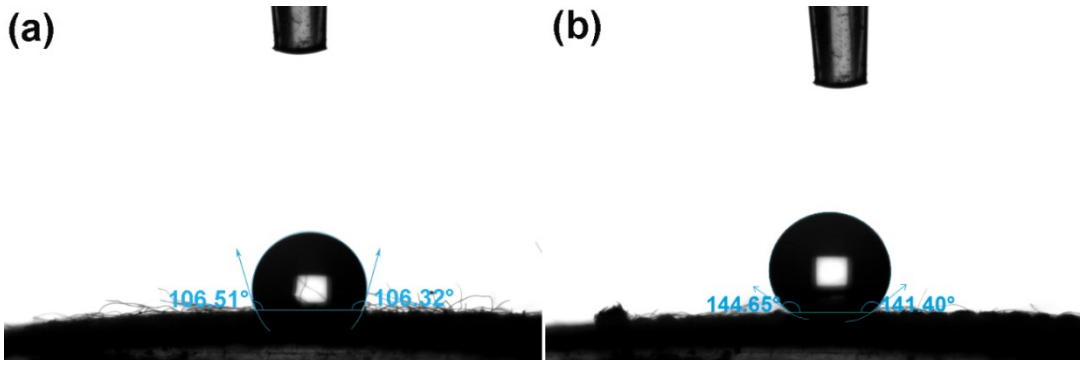

Fig. S20 Water contact angle measurement of (a) Bi-CC and (b) ZIF-8/Bi-CC.

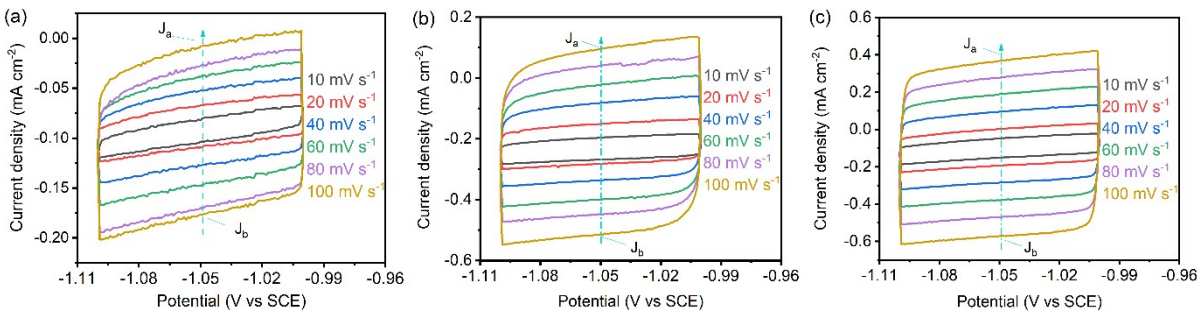

Fig. S21 (a-c) Electrochemically active surface area measurement of CV in the non-faradaic region for ZIF-8/CC, Bi-CC and ZIF-8/Bi-CC. The catalysts' ECSA was calculated using ECSA = C_{dl}/C_s, where C_{dl} is the catalyst's double-layer capacitance, which was determined by the slope of the obtained linear equation of $(J_a - J_b)/2$ and CV scan rates within a nonfaradaic region. Cs stands for the catalyst's specific capacitance, and Cs = 0.030 mF cm^{-2} was adopted in this study.

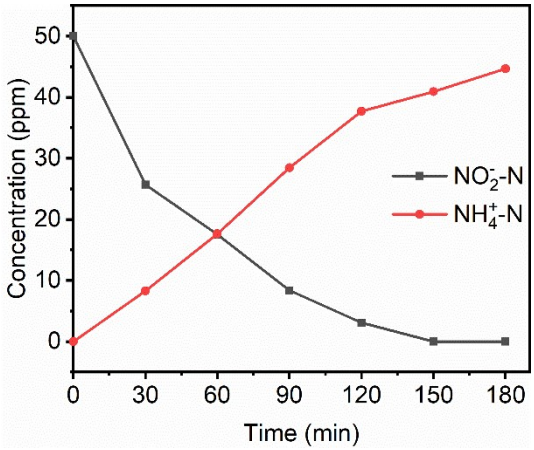

Fig. S22 Electrochemical reduction of $^{NO_2^-}$ - N by ZIF-8/Bi-CC at the current density of 10 mA cm^{-2} in 0.5 M Na_2SO_4 and 50 ppm $^{NO_2^-}$ - N.

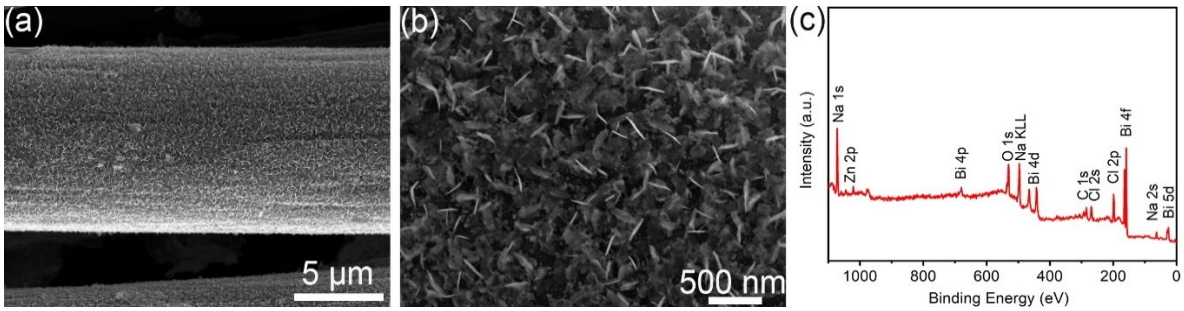

Fig. S23 (a), (b) SEM images with different scales, and (c) full XPS spectrum of the ZIF-8/Bi-CC after long-term tested.

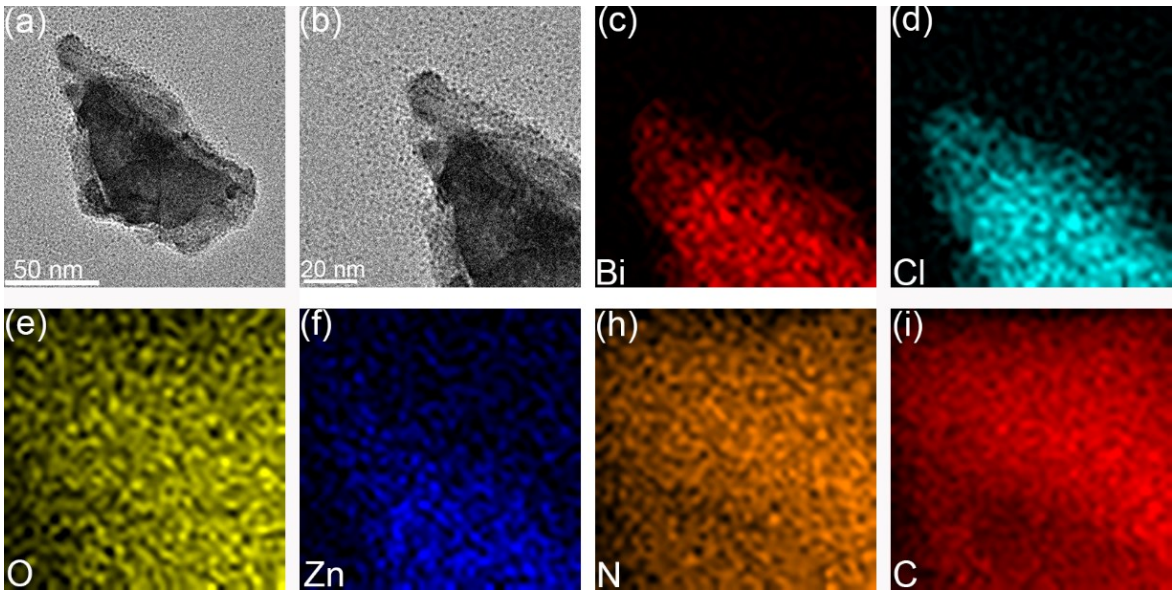

Fig. S24 TEM mapping of nanosheets peel form the tested ZIF-8/Bi-CC after long-term test.

Part Ⅲ：Tables

Table S1. Summary of the BET surface area, C_{dl}, and ECSA of the CC, ZIF-8-CC, Bi-CC and ZIF-8/Bi-CC.

Sample	BET surface area ($m^2 g^{-1}$)	C_{dl} (mF cm^{-2})	ECSA (cm^2)
ZIF-8/CC	17.0	0.8	27.3
Bi-CC	4.0	3.0	99.3
ZIF-8/Bi-CC	30.3	4.6	154.3

Table S2. The energy efficiency of different current density.

Current density (mA cm^{-2})	5	10	15	20
Energy consumption (kwh/kg NO_3^--N)	64.6	73	121.4	176

Table S3. The nitrate reduction reaction process equations

Equations
$NO_3^- + 2H^+ + 2e^- \rightarrow NO_2^- + H_2O$ (S1)
$NO_{3\,(ads)}^- + e^- \rightarrow NO_{3\,(ads)}^{2-}$ (S2)
$NO_{3\,(ads)}^{2-} + H_2O \rightarrow NO_{2\,(ads)}^{\cdot} + 2OH^-$ (S3)
$NO_{2\,(ads)}^{\cdot} + e^- \rightarrow NO_{2\,(ads)}^- + 2H_2O$ (S4)
$NO_{2\,(ads)}^- + e^- \rightarrow NO_{2\,(ads)}^{2-}$(S5)
$NO_{2\,(ads)}^{2-} + H_2O \rightarrow NO_{(ads)} + 2OH^-$ (S6)
$NO_{(ads)} + H^+ + e^- \leftrightharpoons HNO_{(ads)}$(S7)
$HNO_{(ads)} + H^+ + e^- \leftrightharpoons H_2NO_{(ads)}$(S8)
$H_2NO_{(ads)} + H^+ + e^- \leftrightharpoons H_2NOH_{(ads)}$(S9)
$H_2NOH_{(ads)} + H^+ \leftrightharpoons H_3NOH_{(ads)}^+$(S10)
$H_2NOH_{(ads)} + 2H^+ + 2e^- \leftrightharpoons NH_3 + H_2O$ (S11)

Table S4. The composition of the real wastewater (initial PH=6.29)

Ions	Concentration (ppm)
K	$4.13*10^3$
Na	$1.36*10^4$
Ca	47.8
Mg	0.27
Fe	0.03
Ba	0.02
Zn	0.069
Mn	0.74
Ni	0.008
Cl^-	$3.75*10^4$
SO_4^{2-}	24
NO_3^--N	14.5
NH_4^+-N	15.1
Si	0.82
Suspended matter	130
Dissolved solids	$6.45*10^4$

Table S5. Comparison of the NITRR performance among ZIF-8/Bi-CC with other NITRR electrocatalysts

Catalyst	System	Performance	Detecting method	Ref.
ZIF-8/Bi-CC	**Graphite ⎮ 0.5 M Na_2SO_4, 50 ppm NO_3^--N (10 mA cm^{-2})**	**S (NH3): 84.2%**	**UV-Vis spectroscopy**	**This work**
Co_3O_4/Ti	Ir-Ru/Ti ⎮ 0.05 M Na_2SO_4, 50 ppm $NaNO_3$ (10 mA cm^{-2})	S (NH_3): 32%	UV-Vis spectroscopy	1
Co_3O_4/Ti	Ir-Ru/Ti ⎮ 0.5 M Na_2SO_4, 50 ppm NO_3^--N (5.72 mA cm^{-2})	S (NH_3): 80%	UV-Vis spectroscopy	2
Co_3O_4-TiO_2/Ti	Ir-Ru/Ti ⎮ 0.01 M Na_2SO_4, 50 mg L^{-1} $NaNO_3$ (10 mA cm^{-2})	S (NH_3): 80%	UV-Vis spectroscopy	3
Zero valent titanium (ZVT)	ZVT sheet ⎮ 25.9 mg N/L + 12 ppm Cl (2.0 mA cm^{-2})	S (NH_3): 6%	Ion chromatograph	4
Pd–Cu/cAl_2O_3	graphite ⎮ 1000 ppm KNO_3 (10 mA cm^{-2})	S(NH_3): 16.5%	UV-Vis spectroscopy	5
Fe@ N-C	Pt ⎮ 50 mM Na_2SO_4, 50 ppm NO_3^--N (1.3 V vs. SCE)	S (NH_3): <75%	Nessler's reagent	6
Ni-Fe^0/Fe_3O_4	Pt ⎮ 50ppm $NaNO_3$, 10mM NaCl (5 mA cm^{-2})	S(NH_3): 10.44%	UV-Vis spectroscopy	7
$Cu_{50}Ni_{50}$	Pt ⎮ 1 M KOH, 10mM KNO_3 (0V versus RHE)	FE(NH_3): 93% S(NH_3): 81.2%	UV-Vis spectroscopy 1H NMR	8
Cu/Cu_2O	Pt ⎮ 0.5 M Na_2SO_4, 50 ppm NO_3^--N (-0.85V vs RHE)	FE(NH_3): 95.8% S(NH_3): 81.2%	UV-Vis spectroscopy 1H NMR	9
Cu nanosheet	Pt ⎮ 1 M KOH, 10mM KNO_3 (−0.15 V versus RHE)	FE(NH_3):99.7%	UV-Vis spectroscopy ^{1}H NMR	10
TiO_2-x	Pt ⎮ 0.5 M Na_2SO_4, 50 ppm NO_3^--N (-1.6 V vs SCE)	FE(NH_3): 85.0% S(NH_3): 87.1%	UV-Vis spectroscopy ^{1}H NMR	11

Reference in the supporting information

1. L. Su, K. Li, H. Zhang, M. Fan, D. Ying, T. Sun, Y. Wang and J. Jia, *Water Res.*, 2017, **120**, 1-11.
2. C. Li, K. Li, C. Chen, Q. Tang, T. Sun and J. Jia, *Sep. Purif. Technol.*, 2020, **237**.
3. J. Gao, B. Jiang, C. Ni, Y. Qi, Y. Zhang, N. Oturan and M. A. Oturan, *Appl Catal B: Environ*, 2019, **254**, 391-402.
4. F. Yao, Q. Yang, Y. Zhong, X. Shu, F. Chen, J. Sun, Y. Ma, Z. Fu, D. Wang and X. Li, *Water Res.*, 2019, **157**, 191-200.
5. Z. Zhang, Y. Xu, W. Shi, W. Wang, R. Zhang, X. Bao, B. Zhang, L. Li and F. Cui, *Chemical Engineering Journal*, 2016, **290**, 201-208.
6. W. Duan, G. Li, Z. Lei, T. Zhu, Y. Xue, C. Wei and C. Feng, *Water Res*, 2019, **161**, 126-135.
7. Z. A. Jonoush, A. Rezaee and A. Ghaffarinejad, *J. Clean. Prod.*, 2020, **242**.
8. Y. Wang, A. Xu, Z. Wang, L. Huang, J. Li, F. Li, J. Wicks, M. Luo, D. H. Nam, C. S. Tan, Y. Ding, J. Wu, Y. Lum, C. T. Dinh, D. Sinton, G. Zheng and E. H. Sargent, *J. Am. Chem. Soc.*, 2020, **142**, 5702-5708.
9. Y. Wang, W. Zhou, R. Jia, Y. Yu and B. Zhang, *Angewandte Chemie*, 2020, **59**, 5350-5354.
10. X. Fu, X. Zhao, X. Hu, K. He, Y. Yu, T. Li, Q. Tu, X. Qian, Q. Yue, M. R. Wasielewski and Y. Kang, *Appl. Mater. Today*, 2020, **19**.
11. R. Jia, Y. Wang, C. Wang, Y. Ling, Y. Yu and B. Zhang, *ACS Catal.*, 2020, **10**, 3533-3540.